Int. J. Heat Mass Transfer. Vol. 19, pp. 1415–1423. Pergamon Press 1976. Printed in Great Britain

THEORETICAL ANALYSIS OF STEADY AND TRANSIENT OPERATION OF INTERNALLY ENERGISED POROUS ELEMENT UNDER PHASE CONVERSION AND VAPOR SUPERHEAT

DAVID MOALEM and SHIMON COHEN
Department of Fluid Mechanics and Heat Transfer, School of Engineering, Tel-Aviv University, Israel

(*Received* 17 *December* 1975)

Abstract—The major parameters affecting the performance of internally energised porous reactor are theoretically studied under the conditions of phase-conversion and vapor superheat. Thus, three regions: liquid, saturated liquid–vapor mixture and superheated vapor, separated by two phase-change "interfaces" are assumed. The analysis treats a classic hollow cylindrical unit in steady-state and transient operation for a representative range of the viscous flow regime. The study into the transient part of the problem is to follow the "interfaces", in space and time, the exit temperature and the evaporating mass flow rate (or the element heat load). The steady-state solution yields the characteristics in stable operation. The understanding of both the steady and transient solutions leads to a wide insight in determining the significant design parameters and possible areas of improving the performance.

NOMENCLATURE

C_1, C_2, constants of integration (equation 14a);
C_p, specific heat;
$C_{p_{l,v}}$, liquid to vapor specific heat ratio (Cp_l/Cp_v);
D, dimensionless group $(= C_p\dot{m}/2\pi k_T)$;
Ja, Jacob number $[= \lambda\rho_v/Cp_l\rho_l(T_0 - T_i)]$;
k, thermal conductivity;
k_T, effective conductivity of the saturated matrix;
$\dot{m}$, mass flow rate;
$\dot{M}$, dimensionless mass flow rate $[= \dot{m}/\rho\bar{v}(r_o - r_i)]$;
M, dimensionless group, equations (14b);
N, dimensionless rate of heat generation $\left(= \dfrac{q(r_o-r_i)^2}{k_T(T_o-T_i)},\ N_R = \dfrac{N_l(r_o^2-r_i^2)}{(r_o-r_i)^2}\right)$;
p, pressure;
P, dimensionless pressure $[= (p - p_o)/(p_i - p_o)]$;
Pe, Péclet number $[= \bar{v}(r_o - r_i)/\alpha_l]$;
q, rate of heat generation per unit time per unit volume;
r, radial coordinate;
R, dimensionless radial coordinate $[= r/(r_o - r_i)]$;
S, ratio $(= \alpha_T/\alpha_{T,l})$;
t, time;
T, temperature;
T_r, reference temperature $(= T^*)$;
v_r, radial velocity;
$\bar{v}$, overall average Darcy-velocity $\left(= \dfrac{\kappa}{\mu_l}\dfrac{p_i - p_o}{r_i - r_o}\right)$, equation (4);
V, dimensionless Darcy-velocity $(= v_r/\bar{v})$.

Greek symbols

α, thermal diffusivity;
ρ, density;
$\rho_{l,v}$, liquid to vapor density ratio $(= \rho_l/\rho_v)$;
κ, permeability of porous structure;
λ, latent heat of vaporization;
λ_n, eigenvalues;
θ, dimensionless temperature $[= (T - T^*)/(T_o - T_i)]$;
μ, viscosity;
ν, kinematic viscosity $(= \mu/\rho)$;
$\nu_{l,v}$, liquid to vapor kinematic viscosity ratio $(= \nu_l/\nu_v)$;
ε, porosity;
τ, dimensionless time $[= \alpha_{T,l}t/(r_o - r_i)^2]$.

Subscripts

av, average value;
c, start of evaporation;
d, end of evaporation;
f, fluid (liquid or vapor);
i, internal side of cylinder;
l, liquid;
o, external side of cylinder;
r, radial;
t, transient;
T, effective property;
t, l, effective property of matrix saturated with liquid;
v, vapor;
l/v, liquid to vapor ratio;
$*$, saturation state (superscript);
∞, at infinite time (steady-state).

INTRODUCTION

THE CONCEPT of internally energised porous medium is of interest in various application areas. These include nuclear fuel, cladding and shielding, solar collectors, compact regenerator design, Boiling Water Reactor design etc. Also, the short residence time for fluid passing through the porous element is a feature which may lead to its use in various chemical engineering processes.

The present study deals with the use of fluid flow through internally heated porous medium, in particular in connection with the novel methods of energy production. The solid particles forming the porous structure may be nuclear or electrically heated. Heat may be generated also due to the absorption of radiation. The fluid passed through the heated porous medium, may change phase from liquid to vapor and the vapor be further superheated. In particular, where high coolant rates are required, the principle may prove useful due to the minor specific volume and high heat absorbing capacity of a coolant under phase conversion and vapor superheat. The enormous specific surface area enables high specific ratings even with small temperature driving forces between the solid and the fluid.

Internally heated, porous element may also be applied for the production of steam of variable controlled quality (e.g. in food processing and pharmaceuticals).

Most previous studies are related to drying or transpiration cooling systems [1–10], which are usually subjected to a prescribed temperature or heat flux at their surfaces. There appears to be little information available on the important problem of coupled heat and mass transfer in porous media with internal heat generation [3, 11–14]. A steady-state solution of the heat-transfer rates in porous media with temperature-dependent energy source has been recently presented by Moalem [15]. The concept of generating internal heat of a temperature-dependent rate seems to be promising in concern to stability of operation and long-life element due to the dynamic self-control, which such an element possesses.

The present study is an extension of earlier work [15] and constitutes an attempt to evaluate the heat-transfer characteristics of internally heated porous elements in steady and transient operations.

A unit of a hollow porous cylinder is considered, where the flow may be from either the inside or the outside. The liquid feed is firstly heated until its exit temperature reaches saturation. Following this heating period, partial evaporation starts and a phase-change "interface" is thus formed and moves inwardly, while a mixture of saturated liquid and vapor leaves the element. As a complete evaporation is achieved a superheating of the vapor takes place. Thus, two phase-change "interfaces" are assumed to exist in the superheating period, rather than an evaporation front separating a vapor region from the liquid region. The inward phase-change "interface" denotes the average distance where evaporation starts while the external one denotes the average distance where complete evaporation is reached.

The study into the transient part of the problem will be to follow the "interfaces", in space and time, the exit temperature and the mass flow rate (or the element heat load). The steady-state solution will be to yield the variation of the element heat load with the strength of the energy source. The understanding of these is important in predicting the performance of such an element.

THE THEORETICAL MODEL AND GOVERNING EQUATIONS

Consider a unit of a hollow porous cylinder Fig. 1. The inner and outer radii ar r_i and r_o, respectively. Liquid at temperature T_i and pressure P_i is continuously fed to the center of the cylinder. The liquid is assumed to flow radially outwards through the porous medium by an impqsed total pressure gradient $(p_i - p_o)$, where P_o is a constant pressure maintained at the outer

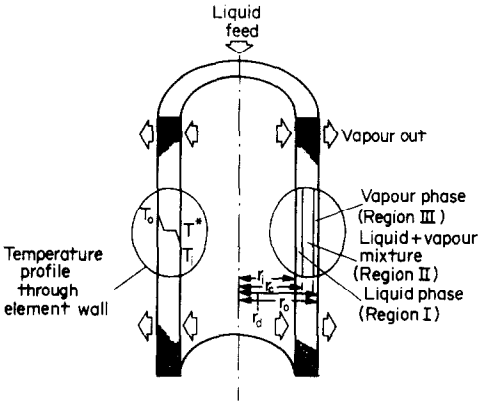

FIG. 1. Schematic presentation of physical system and coordinates.

surface of the cylinder. In the pressure gradients considered here, the flow is slow enough so that the viscous forces dominate over the inertia forces. Because of the complex structure of the porous medium it is impossible to formulate the problem in terms of the actual flow through the pores. Thus, as in most studies on the viscous regime flow through porous medium, the Darcy's law is assumed applicable:

$$v_r = -\frac{\kappa}{\mu_f}\frac{\mathrm{d}p}{\mathrm{d}r} \tag{1}$$

where κ is the permeability of the porous material, μ_f is the fluid viscosity, v_r and $\mathrm{d}p/\mathrm{d}r$ are the radial velocity and the radial pressure gradient, respectively. The use of equation (1) is restricted to a small appropriately defined Reynolds number:

$$(\rho v d/\mu) < 1$$

where d denotes an average pore diameter.

Under transient conditions, a modified Darcy's law is sometimes used [16, 17] in the form:

$$\frac{\partial v}{\partial t} + \frac{v}{\kappa}v = -\frac{1}{\rho_f}\frac{\partial P}{\partial r}$$

where ρ_f is the fluid density and κ/v is the viscous time. The latter, except for the first fraction of second is small enough so that the term $\partial v/\partial t$ may be neglected.

Energy is generated in the medium at an arbitrary volumetric rate q. After time interval t_i^* (measured from the start-up of the heat generation) the temperature at the outlet side reaches the boiling point of the liquid, and evaporation may take place within the medium. If the rate of heat generation is large enough the liquid feed is completely converted to saturated

vapor (at time t_v^*) and the saturated vapor is further superheated until steady-state is reached. It is assumed that the regions of different phases are "separated" by two phase-change "interfaces", the first of which (at r_c) denotes the average distance where evaporation starts and the second (at r_d) denotes the average distance where complete evaporation is reached. The liquid passed through the heated porous medium, is firstly heated to saturation state in region I, changes phase from liquid to vapor in region II, and the vapor is further superheated in region III to an exit temperature T_o, greater than the saturation temperature of the liquid corresponding to the pressure p_o. The temperature and pressure at the evaporation region are the saturation temperature and pressure T^* and p^* respectively, where $p_o < p^* < p_i$ and $T^*(p_i) < T^*(p^*) < T^*(p_o)$. For the case under consideration where equation (1) is applicable, the total pressure gradient is relatively small. Hence, $T^*(p_i) \approx T^*(p_o)$, and the saturation temperature at p^* is firstly approximated by $T^*(p_i + p_o/2)$, and is corrected by solving for the pressure distribution.

Consistent with slow flow through the porous medium it is reasonable to assume that the temperature of the solid and the adjacent fluid are equal. Thus the heterogeneous solid–fluid system is treated as a continuum, which allows average or "macroscopic" governing equations to be applied. In order to apply an average energy equation, it is necessary to determine an effective thermal conductivity of the saturated porous medium. Hashin and Shtrikman [18] derived an equation for the upper and lower bounds of the effective conductivity of heterogeneous materials, and [19–23] discussed the prediction of effective conductivities. For the problem under consideration, the upper bound from [18] is utilized to evaluate the effective conductivity for the saturated matrix (taking an upper and lower bound will yield limits on the solution of the problem). The average energy equation can be written in the form [7, 16]:

$$(\rho C_p)_T \frac{\partial T}{\partial t} + \rho_f C_{pf} v \frac{\partial T}{\partial r} = \frac{\partial}{\partial r}\left(k_T \frac{\partial T}{\partial r}\right) + q \qquad (2)$$

where q is the rate of heat generated within the porous structure per unit time per unit volume, k_T and $(\rho C_p)_T$ are the effective conductivity and heat capacity of saturated matrix. Consisting with assuming equal fluid and solid temperatures, the latter is given by:

$$(\rho C_p)_T = (1-\varepsilon)(\rho C_p)_{\text{solid}} + \varepsilon(\rho C_p)_{\text{fluid}}$$

where ε is the porosity of the matrix.

The equation of continuity may be written in the form [16, 24]

$$\varepsilon \frac{\partial \rho_f}{\partial t} + \frac{\partial(\rho_f r v_r)}{\partial r} = 0 \qquad (3)$$

with f denotes for the fluid.

We now define the following dimensionless variables:

$$R = r/(r_o - r_i),\ P = (p - p_o)/(p_i - p_o),\ \theta = (T - T^*)/(T_o - T_i)$$

$$\bar{v} = -\frac{\kappa}{\mu_l}\frac{p_i - p_o}{r_i - r_o} \quad V = v/\bar{v}, \quad \dot{M} = \dot{m}/[\rho \bar{v}(r_o - r_i)]$$

$$Ja = \frac{\lambda \rho_v}{Cp_l \rho_l (T_o - T_i)}, \quad Pe = \frac{\bar{v}(r_o - r_i)}{\alpha_l}, \quad \tau_T = \frac{\alpha_{T,l} t}{(r_o - r_i)^2}$$

$$D = \frac{C_p \dot{m}}{2\pi k_T}, \quad N = \frac{q(r_o - r_i)^2}{(T_o - T_i)k_T}, \quad N_R = \frac{N(R_i - R_o)}{R_o - R_1}$$

$$\rho_{l,v} = \rho_l/\rho_v, \quad \nu_{l,v} = \nu_l/\nu_v, \quad Cp_{l,v} = Cp_l/Cp_v$$

$$\alpha_T = \frac{k_T}{(\rho C_p)_T}, \quad \alpha_{T,l} = \frac{k_{T,l}}{(\rho C_p)_{T,l}}, \quad S = \alpha_T/\alpha_{T,l} \qquad (4)$$

where the subscripts l, v refer to liquid and vapor respectively, T to an overall effective property of fluid and solid and (T, l) refer to an overall effective property of the matrix saturated with liquid. With reference to the above, the continuity, motion and energy equations are transformed to dimensionless forms:

$$\frac{\partial}{\partial R}(VR) = 0 \qquad (5)$$

$$V = -\frac{dP}{dR} \qquad (6)$$

$$S\frac{d\theta}{d\tau} = \frac{d^2\theta}{dR^2} + \frac{1-D}{R}\frac{d\theta}{dR} + N \qquad (7)$$

where $S = 1$ is for the liquid region and $S = \alpha_T/\alpha_{T,l}$ is for the vapor region.

The initial value and the boundary conditions applicable to this problem are:

$$R_i \leqslant R \leqslant R_o, \quad P = P(R), \quad \theta = \theta_i, \quad \tau \leqslant 0 \qquad (8a)$$

$$R = R_i, \quad P = 1.0, \quad \theta = \theta_i, \quad \tau > 0 \qquad (8b)$$

$$R = R_c(\tau) \text{ or } R_d(\tau), \quad P = P^*, \quad \theta = 0, \quad \tau > 0 \qquad (8c)$$

and either of:

$$R = R_o, \quad P = 0, \quad \frac{d^2\theta}{dR^2} = 0, \quad \tau > 0 \qquad (8d')$$

$$R = R_o, \quad P = 0, \quad \theta = \theta_o, \quad \tau > 0 \qquad (8d'')$$

$$R = R_o, \quad P = 0, \quad \frac{d\theta}{dR} = 0, \quad \tau > 0 \qquad (8d''')$$

where R_c and R_d are the dimensionless phase-change "interfaces" position, (see Fig. 1).

Acutally, because of the thermal conductivity of the fluid, the fluid temperature will probably rise slightly before it enters at $R = R_i$. However, the dispenser which is usually placed before the heated porous element reduces the effect of the heated solid on the inlet temperature of the incoming feed. Also, the heat transfer to the surroundings by radiation and convection from the shown-side of the element is negligible. Solutions with either of (8d) are almost identical. In a previous study [15] the steady heat losses were found to be 2–3% of the total heat generation. Some higher value (8%) was reported by [25]. Thus, either of (8d) is used with constant inlet temperature, θ_i, at $R = R_i$. Constant temperature at the outer-radius, R_o, can be maintained by the external vapor chamber. The evaporation in the intermediate region is assumed to proceed at constant temperature and pressure. This is reasonably valid in the case under consideration, where the total pressure gradient is by itself relatively small.

(A) *Steady-state operation*

Solution for the mass flux. The solution for the mass flux may analytically be obtained by assuming constant properties. This assumption is reasonable under the conditions of low superheat and small pressure gradient.

Substituting equation (6) into (5) and integrating, using the boundary-conditions in equation (8) yield the pressure distribution in the liquid and vapor regions:

$$P_l = 1-(1-P^*)\frac{\ln(R/R_i)}{\ln(R_c/R_i)} \tag{9a}$$

$$P_v = P^*\frac{\ln(R/R_o)}{\ln(R_d/R_o)}. \tag{9b}$$

The mass flux in each region is given by:

$$\dot{m} = 2\pi r v_f \rho_f \tag{10a}$$

or in dimensionless form:

$$\dot{M} \equiv \frac{\dot{m}}{\bar{v}\rho_f(r_o-r_i)} = 2\pi VR \tag{10b}$$

where v_f (or V) is the Darcy velocity as is defined by equation (1) [or equation (6)] and by the local pressure gradient ($\mathrm{d}p/\mathrm{d}r$). When the latter is evaluated from either of equations (9) and is combined with equations (6) and (10b) the following are obtained:

$$\dot{M}_l \equiv \frac{\dot{m}_l}{\bar{v}_l\rho_f(r_o-r_i)} = 2\pi\frac{1-P^*}{\ln(R_c/R_i)} \tag{11a}$$

$$\dot{M}_v \equiv \frac{\dot{m}_v}{\bar{v}_v\rho_v(r_o-r_i)} = 2\pi\frac{P^*}{\ln(R_o/R_d)}. \tag{11b}$$

Since steady-state is considered the mass fluxes in the liquid and vapor regions are identical. Equating equations (11a) and (11b) yields the saturation pressure:

$$P^* = \frac{\ln(R_o/R_d)}{\ln(R_c/R_i)+\ln(R_o/R_d)}. \tag{12}$$

Equation (12) is used now to eliminate P^* in either of equations (11). This yields the dimensionless mass flux:

$$\dot{M}_l = \dot{M}_v = 2\pi/[\ln(R_c/R_i)+\ln(R_o/R_d)]. \tag{13}$$

Note that once the "interfaces" position R_c and R_d are evaluated, equations (9) and (13) may be used to evaluate the pressure distributions and the mass flux through the porous medium.

Solution of the energy equation. In the case under consideration, equation (7) reduces to a linear equation of first order. Its solution is given by:

$$\theta = C_1\frac{R^D}{D} - MR^2 + C_2 \tag{14a}$$

where:

$$M = \begin{cases} \frac{1}{2}\dfrac{N}{2-D} & \text{if } D \neq 2 \\ \dfrac{N}{2}(\ln R - \frac{1}{2}) & \text{if } D = 2. \end{cases} \tag{14b}$$

The constants of integration C_1 and C_2 are now evaluated for each of the liquid vapor regions by introducing the boundary-conditions as in equations (8). With (8d″) and $D \neq 2$ this yields:

$$\theta_l = \left[-\theta_i + M_l(R_c^2-R_i^2)\right]\frac{R^{D_l}-R_i^{D_l}}{R_c^{D_l}-R_i^{D_l}} - M_l(R^2-R_i^2)+\theta_i, \quad D \neq 2 \tag{15a}$$

$$\theta_v = \left[\theta_o + M_v(R_o^2-R_d^2)\right]\frac{R^{D_v}-R_d^{D_v}}{R_o^{D_v}-R_d^{D_v}} - M_v(R^2-R_d^2), \quad D \neq 2 \tag{15b}$$

where M is as defined in (14b). The corresponding expressions for $D = 2$ are:

$$\theta_l = \left[-\theta_i + \frac{N}{2}\left(R_c^2\ln R_c - \frac{R_c^2}{2} - R_i^2\ln R_i + \frac{R_i^2}{2}\right)\right]\frac{R^2-R_i^2}{R_c^2-R_i^2} - \frac{N}{2}\left(R^2\ln R - \frac{R^2}{2} - R_i^2\ln R_i + \frac{R_i^2}{2}\right)+\theta_i, \quad D = 2 \tag{15c}$$

$$\theta_v = \left[\theta_o + \frac{N}{2}\left(R_o^2\ln R_o - \frac{R_o^2}{2} - R_d^2\ln R_d + \frac{R_d^2}{2}\right)\right]\frac{R^2-R_d^2}{R_o^2-R_d^2} - \frac{N}{2}\left(R^2\ln R - \frac{R^2}{2} - R_d^2\ln R_i + \frac{R_d^2}{2}\right)+\theta_i, \quad D = 2. \tag{15d}$$

The analogue solutions based on (8d′) or (8d‴) may easily be obtained in a similar way.

(B) *Transient solution*

Based on the fact that as $\tau \to \infty$, the system approaches a steady state, the transient solution is split into a limiting solution, $\theta_\infty(R)$ at $\tau \to \infty$ and a transient function, $\theta_t(R,\tau)$:

$$\theta(R,\tau) = \theta_\infty(R) - \theta_t(R,\tau). \tag{16}$$

Introducing equation (16) into (7) yields:

$$\frac{\mathrm{d}\theta_t}{\mathrm{d}\tau} = \frac{1-D}{R}\frac{\mathrm{d}\theta_t}{\mathrm{d}R} + \frac{\mathrm{d}^2\theta_t}{\mathrm{d}R^2}. \tag{17}$$

The general solution of equation (17) is

$$\theta_t(R,\tau) = \sum_{n=1} C_n R^{D/2} Z_{D/2}(\lambda_n R)\exp(-\lambda_n^2\tau/S) \tag{18}$$

where the cylindrical function Z is a linear combination of the Bessel functions of the first and second kind and of order $D/2$:

$$Z_{D/2}(\lambda_n R) = C_1 J_{D/2}(\lambda_n R) + C_2 Y_{D/2}(\lambda_n R). \tag{19}$$

The appropriate boundary-conditions for θ_t are obtained by combining equation (8) with equation (16). The constants and eigenvalues are now evaluated according to the conditions at the boundaries of each region:

Firstly, the liquid is heated until the exit temperature (at R_o) reaches the saturation point. In this time-interval, denoted here as the heating period, the temperature difference between the porous element and its environment is relatively small, hence equation (8d‴) is assumed to hold. With

$$C_1 = Y_{D_l/2}(\lambda_n R_i) \quad \text{and} \quad C_2 = -J_{D_l/2}(\lambda_n R_i) \tag{20a}$$

the function θ_t satisfies the condition at the liquid entry, equation (8b). The corresponding eigenvalues λ_n, are

the positive roots of the characteristic equation [obtained from equation (8d‴)]:

$$J_{(D_l/2)-1}(\lambda_n R_o) Y_{D_l/2}(\lambda_n R_i) - J_{D_l/2}(\lambda_n R_i) Y_{(D_l/2)-1}(\lambda_n R_o) = 0. \quad (20b)$$

In the superheating period, when two phase-change "interfaces" exist the appropriate boundary-conditions for each region are similarly used:
For the liquid region again

$$C_1 = Y_{D_l/2}(\lambda_n R_i) \quad \text{and} \quad C_2 = -J_{D_l/2}(\lambda_n R_i) \quad (21a)$$

while the characteristic equation

$$J_{D_l/2}(\lambda_n R_c) Y_{D_l/2} - J_{D_l/2}(\lambda_n R_i) Y_{D_l/2}(\lambda_n R_c) = 0 \quad (21b)$$

is now obtained from the condition at $R = R_c$.

Similarly, with

$$C_1 = Y_{Dv/2}(\lambda_n R_o), \quad C_2 = -J_{Dv/2}(\lambda_n R_o) \quad (22a)$$

and

$$J_{Dv/2}(\lambda_n R_d) Y_{Dv/2}(\lambda_n R_o) - J_{Dv/2}(\lambda_n R_o) Y_{Dv/2}(\lambda_n R_d) = 0 \quad (22b)$$

the conditions at the boundaries of the superheating region are satisfied.

Applying now the orthogonality of the cylindrical function with the initial condition $\theta_l(0, R) = \theta_\infty(R) - \theta_i$ yields the constants C_n:

$$C_n = \frac{\int \theta_l(R, 0) R^{1-D/2} Z_{D/2}(\lambda_n R)\, dR}{\int [Z_{D/2}(\lambda_n R)]^2 R\, dR}. \quad (23)$$

Note that the integrations in equation (23) are carried out with the use of formula given in [26] and in the appropriate instantaneous range of either liquid or the vapor phase. Also, equations (20b, 21b, 22b) are numerically solved.

CALCULATION PROCEDURE AND PRESENTATION OF CALCULATED RESULTS

The main parameters affecting the performance of such an element are (a) the rate of heat generation within the solid, (b) the rate of flow of working fluid, (c) the degree of pre-heating of the incoming liquid feed and (d) the degree of superheat of outcoming vapor. These are presented in the following for a constant rate of heat generation. However, since the results are obtained numerically, it is interesting to note the point values of the basic variables R_c, R_d and the temperature profiles through the various regions.

To have a clear idea of the results obtained we shall consider, as an example, water as a working fluid and a hollow cylindrical porous element of a constant porosity (= 0.39) and inner and outer radii of 1.0 cm and 2.0 cm. Thus the dimensionless radii R_i, R_o are 1.0 and 2.0 respectively.

The pressure distribution (equations 9), the mass flux (equation 13) and the temperature profiles (equations 15) require the values of R_c and R_d. These are evaluated by utilizing the following energy balances on the different regions of the element:

$$\left(\dot{m}_l - 2\pi\varepsilon\rho_l r_c \frac{dr_c}{dt}\right) h_l^* - \dot{m}_l h_l^i - \pi q(r_c^2 - r_i^2) - 2\pi k_{T,l} r \frac{dt}{dr}\bigg|_{r=ri} \quad (24a)$$

$$\left(\dot{m}_v - 2\pi\varepsilon\rho_v r_d \frac{dr_d}{dt}\right) h_v^* - \left(\dot{m}_l - 2\pi\varepsilon\rho_l r_c \frac{dr_c}{dt}\right) h_l^* = \pi q(r_d^2 - r_c^2) + 2\pi k_{T,v} r \frac{dt}{dr}\bigg|_{r=r_d} \quad (24b)$$

$$\dot{m}_v h_v^o - \left(\dot{m}_v - 2\pi\varepsilon\rho_v r_d \frac{dr_d}{dt}\right) h_v^* = \pi q(r_o^2 - r_d^2) - 2\pi k_{T,v} r \frac{dT}{dr}\bigg|_{r=r_d} \quad (24c)$$

$$\dot{m}_v h_v^o - \dot{m}_l h_l^i = \pi q(r_o^2 - r_i^2) - 2\pi k_{T,l} r \frac{dT}{dr}\bigg|_{r=ri} \quad (24d)$$

where h denotes enthalpy and superscripts i, o, * refer to inlet, outlet and saturation temperature, respectively. Note that only three of the above relationships are independent. These may be simplified by neglecting the conduction fluxes ($= -k_T\, dT/dr$) at the boundaries r_i, r_c, r_d and r_o. Exact calculations by one of the authors [15] show that the boundary fluxes are fairly small compared to the rate of heat generated within region I where the liquid is heated to saturation, and region II where the saturated liquid evaporates. Reasonable accuracy (1.25–2.6%) was achieved by utilizing the energy balances over these two regions, combined with the overall energy balance.

Calculation procedure for transient operation

The calculation procedure for transient operation is as follows: Firstly, the liquid is heated while it passes through the heated element, until the exit temperature at R_o reaches the saturation temperature, T^* at time $t = t_l^*$. For all $t < t_l^*$ use is made of equations (18)–(20) in calculating the transient temperature profiles.

As the liquid reaches saturation at R_o, partial evaporation starts. The first phase-change "interface", R_c is now formed and starts to move inwardly, while a mixture of saturated liquid and vapor leaves the element at R_o. Integration of equation (24a) (with $R_d = R_o$) yields the variation of the interface, R_c with space and time. Simultaneously, an overall heat balance [similar to equation (24d)] yields the quality of the saturated mixture at the exit. Calculation proceeds until a complete evaporation is achieved. At this point, t_v^* superheating of the saturated vapor starts.

As superheating of vapor takes place one more equation is available (equation 24c), which is used now to evaluate the corresponding R_d. Note that the variation of R_d with time is relatively small in this interval and dR_d/dt can be neglected or averaged in equation (24) in order to facilitate the computation. The small variation of R_d with time is substantiated by the fact that the value of R_d (at steady state) is very close to R_o for low and intermediate superheat [15].

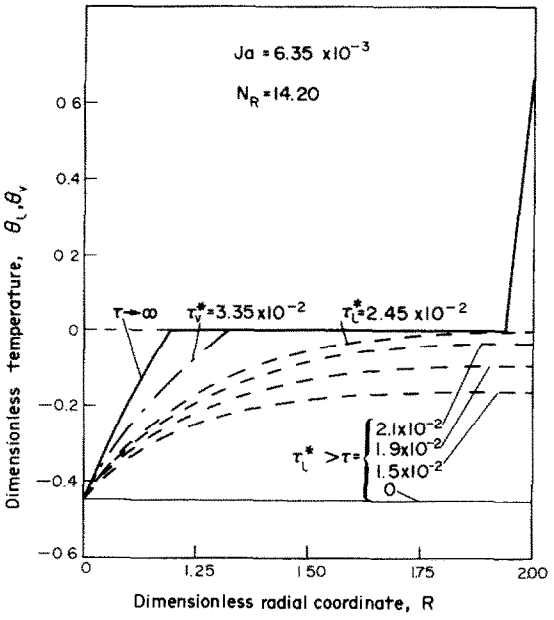

FIG. 2. Development of temperature profile for $Ja = 6.35 \times 10^{-3}$, $N_R = 14.20$.

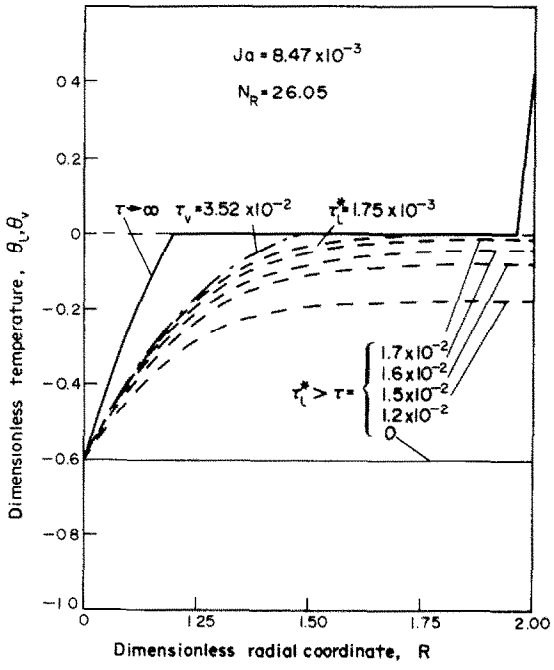

FIG. 3. Development of temperature profile for $Ja = 8.47 \times 10^{-3}$, $N_R = 26.05$.

Figures 2–4 demonstrate the transient temperature profiles for various time intervals before the liquid reaches its saturation point ($t < t_l^*$), at time the liquid reaches saturation ($t = t_l^*$) and at time saturated vapor is obtained ($t = t_v^*$). Also included in the figures are the steady-state profiles. The two parameters being changed are the Jacob number which represents an indication for the overall temperature difference ($T_o - T_i$) and the required degree of superheating at steady-state operation, θ_o.

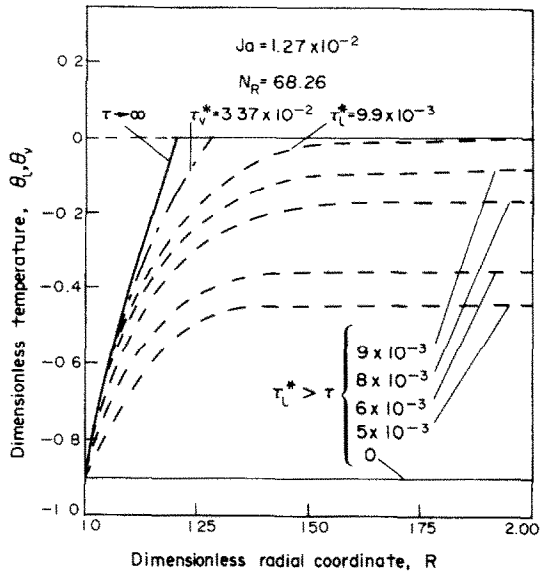

FIG. 4. Development of temperature profile for $Ja = 1.27 \times 10^{-2}$, $N_R = 68.26$.

Note that the intersection of the temperature profile at $t = t_v^*$ with the line of $\theta = 0$ represents the position of the inward phase-change "interface" ($R = R_c$) at the moment the superheating region is just starting to build up ($R_d = 1.0$). The corresponding intersections of the steady-state curve denote the values of R_c and R_d when the three regions are steadily established to yield the required degree of superheat, θ_o. As is indicated in the figures, the superheating region is larger for higher degree of superheat.

In view of equation (13) the possible mass flux through the porous element is determined by the position of the two phase-change "interfaces", R_c and R_d. The variation of these with the dimensionless time and the corresponding variation of the simultaneous mass flux are presented as an example for $Ja = 8.4710^{-3}$ in Figs. 5 and 6. As is indicated in Fig. 6, the flux is constant in the preheating period ($t < t_l^*$) and is rapidly increasing due to the fast inward movement of the liquid phase interface, R_c at $t > t_l^*$ (see Fig. 5). At $t = t_v^*$ the rate of variation of R_c is relatively small, while the mass flux starts decreasing due to the pressure gradient which is now developed in the third superheating region.

The dimensionless temperature at the outlet $\theta(\tau, R_o)$ is normalized now with reference to its value at steady-state conditions, θ_o and the variation (Fig. 7) of the fraction $\theta(\tau, R_o)/\theta_o$ is plotted with the dimensionless time for various operating conditions. Note that the approach of that fraction to unity represents the approach of system performance to steady-state operation.

Steady-state operation

In steady-state operation ($dR_c/dt = dR_d/dt = 0$), one can easily eliminate R_d from the first two of equations (24):

$$R_d = [R_c^2 - \rho_{l,v} Ja(R_c^2 - R_i^2)/\theta_i]^{\frac{1}{2}}. \qquad (25)$$

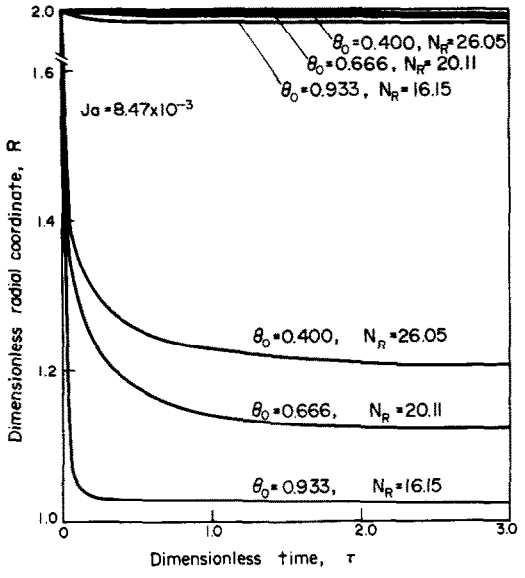

FIG. 5. Instantaneous position of the two phase-conversion "interfaces" for $Ja = 8.47 \times 10^{-3}$ at various N_R.

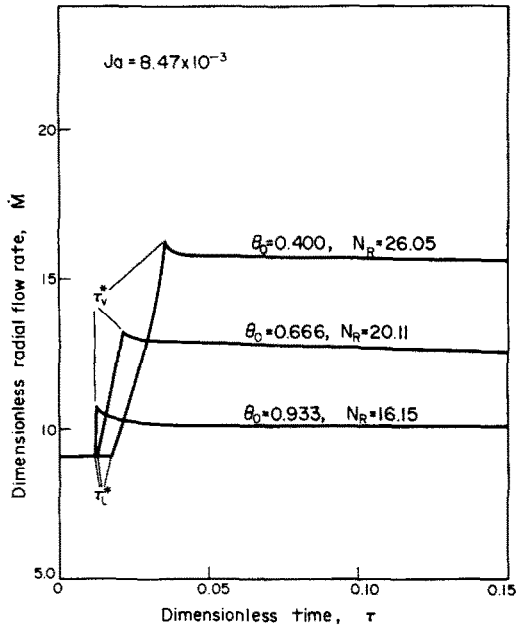

FIG. 6. Variation of radial mass flow rate with time for $Ja = 8.47 \times 10^{-3}$ at various N_R.

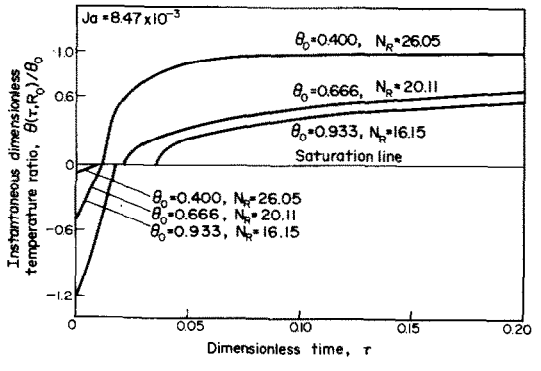

FIG. 7. Variation of the outlet temperature with time for $Ja = 8.47 \times 10^{-3}$ at various N_R.

Substituting M and R_d into equation (24d) yields:

$$\frac{\theta_o}{C_{Pl,v}} - \theta_i + Ja\rho_{l,v} - \frac{1}{2}\frac{N_l}{Pev_{l,v}}\frac{R_o+R_i}{R_o-R_i} \times \{\ln[R_o/R_c^2 - \rho_{l,v}Ja(R_c^2-R_i^2)/\theta_i)] - v_{l,v}\ln(R_c/R_i)\} = 0. \quad (26)$$

Starting with initial guess for R_c, equation (25) is used to evaluate R_d. Based on these R_c, R_d values, the corresponding q (or N) is calculated by equation (24b). The calculated N is inserted into equation (26), the solution of which yields a new value of r_c which is compared with the previous one, until convergence is achieved.

Figure 8 represents the dimensionless radial distance of the two phase-change "interfaces" for various degrees of superheat and various values of Jacob number. Note that as $\theta_o \to 0$ (or $\theta_i \to -1.0$) the outcoming vapor is at saturation temperature T^*, and hence $R_d \to R_o$. As $\theta_o \to 1.0$ (or $\theta_i \to 0$) the incoming liquid is at the saturation temperature T^*, and hence $R_c \to R_i$.

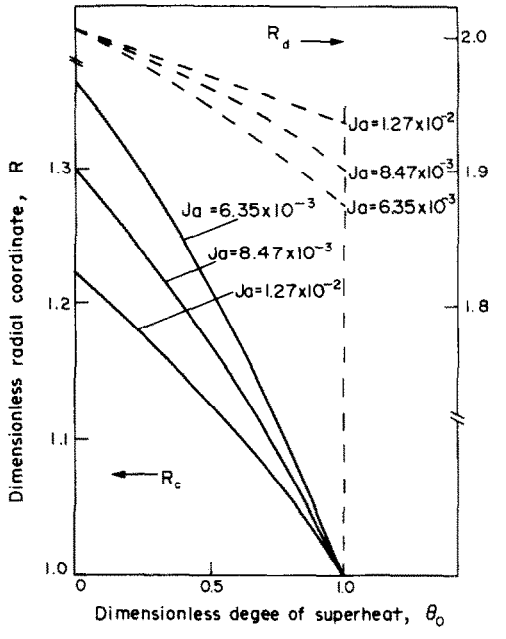

FIG. 8. Steady position of the two phase-conversion "interfaces" for various parameters.

The corresponding variation of the dimensionless mass flux with the degree of superheat is shown in Fig. 9. Also included in these figures the dimensionless rate of heat generation, N_R. As the degree of superheat is increased, the phase-change "interface", R_d, moves inside while R_c remains almost unchanged. Thus, the mass flux and hence the required rate of heat generation should both decrease (see equation 13). Similarly, for low superheat, the increase in R_c brings about a corresponding increase in the mass flux.

The mass flux and the rate of heat generation determine the values of the dimensionless groups D and N which appear in the temperature profiles. Typical steady temperature profiles for high, low and intermediate superheat are represented in Fig. 10. Note that,

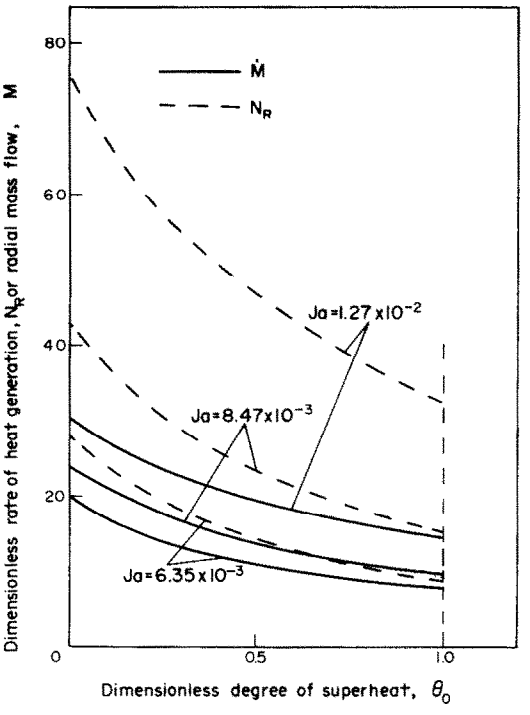

FIG. 9. Interrelations between major operating parameters (N_R, θ_o, $\dot{M}$, Ja) of an internally energised porous reactor.

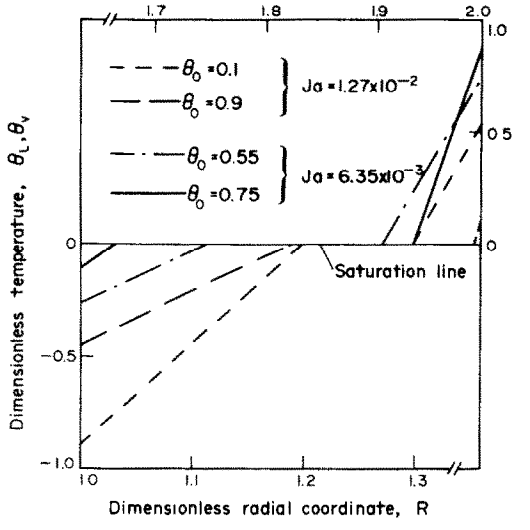

FIG. 10. Steady-state temperature profiles within the porous element for various parameters.

θ_l denotes the temperature variation in the liquid heating region and θ_v corresponds to the temperature variations in the superheating region. The intersection of θ_l and θ_v curves with the saturation line ($\theta = 0$) indicates the values of R_c and R_d, respectively.

FINAL REMARKS

A theoretical analysis of internally energised porous reactor has been presented. The analysis is applicable for predicting the characteristics of a porous reactor producing vapor where small quantities of variable controlled superheatings are required. The principle may also be applied for cooling of nuclear particles by evaporating high latent-heat fluid while flowing through the particles bed.

The study presented here is restricted to low flow rates of coolant through the porous medium. An extended analysis for high flow rates and a temperature-dependent heat-generation rate is now underway.

REFERENCES

1. P. Grootenhuis and N. P. W. Moor, Some observations of the mechanism of sweat cooling, *Proc. 7th Int. Congr. Applied Mechanics*, Vol. 3, pp. 106–119 (1948).
2. S. Weinbaum and H. L. Wheeler, Jr., Heat transfer in sweat-cooled porous metals, *J. Appl. Phys.* **20**, 113–122 (1949).
3. L. Green, Jr., Gas cooling of a porous heat source, *J. Appl. Mech.* **19**(2), 173–178 (1952).
4. E. Meyer and A. Bartos, Transpiration cooling in porous metal wall, *Jet Propul.* **24**(b), 366–368 (1954).
5. J. C. Y. Koh and E. P. del Casal, Heat and mass flow through porous matrices for transpiration cooling, in *Proc. 1965 Heat Transfer and Fluid Mechanics Inst.*, edited by A. C. Charwat, Stanford Univ. Press, Stanford, CA (1965).
6. J. C. Y. Koh and E. P. del Casal, Two-phase flows in porous matrices for transpiration cooling, in *Developments in Mechanics*, edited by J. E. Cermak and J. R. Goodman. Colorado State University (1968).
7. J. C. Y. Koh, J. F. Price and R. Colony, On a heat and mass transfer problem with two moving boundaries, in *Progress in Heat and Mass Transfer*, Vol. 11, edited by T. F. Irvine, Jr., W. E. Ibele, J. P. Harnett and R. J. Goldstein. Pergamon Press, Oxford (1969).
8. J. R. Schuster and T. G. Lee, Application of an improved transpiration cooling concept to space shuttle type vehicles, *J. Spacecraft* **9**(11), 804 (1972).
9. A. Rubin and S. Schweitzer, Heat transfer in porous media with phase change, *Int. J. Heat Mass Transfer* **15**, 43 (1972).
10. S. Schweitzer, Multivalued relations between surface conduction and surface temperature in a saturated porous media with phase change, *Int. J. Heat Mass Transfer* **16**, 1496 (1973).
11. J. P. Chion and M. M. El-Wakil, Heat transfer and flow characteristics of porous matrices with radiation as a heat source, *J. Heat Transfer* 69 (1966).
12. D. W. Lyons and J. P. Hatcher, Drying of a porous medium with internal heat generation, *Int. J. Heat Mass Transfer* **15**, 897 (1972).
13. R. J. Raiff and P. C. Wayner, Evaporation from a porous flow control element on a porous heat source, *Int. J. Heat Mass Transfer* **16**, 1919 (1973).
14. G. B. Melese-d'Hospital and J. E. Wilkins, Steady-state heat conduction inslabs, cylindrical and spherical shells with non-uniform heat generation, *Nucl. Engng Design* **24**, 71 (1973).
15. D. Moalem, Steady state heat transfer within porous medium with temperature dependent heat generation, *Int. J. Heat Mass Transfer* **19**(5), 529 (1976).
16. M. Combarnous and B. LeFur, Convection mixte dans une couche poreuse horizontale, in *Proceedings of the Fourth International Heat Transfer Conference, Paris*, Vol. VII, paper CT 3.3, A.I.Ch.E., New York (1970).
17. J. Boer, D. Zaslavsky and S. Irmay, *Physical Principles of Water Percolation and Seepage*, p. 78. UNESCO, Paris (1968).
18. Z. Hashin and S. Shtrikman, Note on the effective constants of composite materials, *J. Franklin Inst.* **271**, 423–426 (1961).
19. D. Kunii and J. M. Smith, Heat transfer characteristics of porous rocks, *A.I.Ch.E. Jl* **6**, 71–77 (1960).

20. R. L. Gorring and S. W. Churchill, Thermal conductivity of heterogeneous materials, *Chem. Engng Prog.* **57**, 53–59 (1961).
21. W. Woodside and J. H. Messmer, Thermal conductivity of porous media, *J. Appl. Phys.* **32**, 1688–1706 (1961).
22. D. Kunii and M. Suzuki, Particle-to-fluid heat and mass transfer in packed beds of fine particles, *Int. J. Heat Mass Transfer* **10**, 845–852 (1967).
23. A. V. Luikov, A. G. Shashkov, L. L. Vasiliev and Y. E. Fraiman, Thermal conductivities of porous systems, *Int. J. Heat Mass Transfer* **11**, 117–140 (1968).
24. A. E. Scheidegger, *Physics of Flow Through Porous Media.* Macmillan, New York (1960).
25. W. U. Choudhury and M. M. El-Wakil, Heat transfer and flow characteristics in conductive porous media with energy generator, in *Proceedings of the Fourth International Heat Transfer Conference, Paris–Versailles*, Paper CT. 32. A.I.Ch.E., New York (1970).
26. E. Janke and F. Emde, *Tables of Functions.* Dover, New York (1945).

ANALYSE THEORIQUE DU FONCTIONNEMENT STATIONNAIRE ET TRANSITOIRE D'UN ELEMENT POREUX AVEC APPORT INTERNE D'ENERGIE EN PRESENCE DE CHANGEMENT DE PHASE ET DE VAPEUR SURCHAUFFEE

Résumé—Les principaux paramètres qui agissent sur le fonctionnement d'un réacteur poreux avec apport interne d'énergie sont étudiés théoriquement dans des conditions de changement de phase et de vapeur surchauffée. Ainsi, on distingue trois régions: le liquide, le mélange liquide–vapeur saturée, la vapeur surchauffée, séparées par deux "interfaces" de changement de phase.

L'analyse traite d'une unité cylindrique creuse classique en fonctionnement stationnaire et transitoire dans un domaine représentatif du régime visqueux. L'étude de la partie transitoire du problème consiste à suivre les "interfaces" dans l'espace et dans le temps, la température de sortie et le taux d'évaporation (ou la chaleur contenue dans l'élément). La solution stationnaire fournit les caractéristiques en fonctionnement stable. La compréhension de ces deux régimes permet de donner un éclairage nouveau à la détermination des paramètres significatifs de construction et des domaines possibles d'amélioration des performances.

THEORETISCHE ANALYSE STATIONÄRER UND INSTATIONÄRER VORGÄNGE IN PORÖSEN KÖRPERN MIT WÄRMEQUELLEN BEI PHASENUMWANDLUNG UND DAMPFÜBERHITZUNG

Zusammenfassung—Die Hauptparameter, die das Verhalten poröser Reaktionskörper mit Wärmequellen beeinflussen, werden theoretisch untersucht unter der Bedingung von Phasenumwandlung und Dampfüberhitzung. Es werden drei Bereiche postuliert: Flüssigkeit, gesättigtes Flüssigkeits—Dampfgemisch und überhitzter Dampf: sie sind durch zwei Phasenänderungsschichten getrennt.

In der Analyse wird die klassische Hohlzylindereinheit bei stationärer und instationärer Arbeitsweise behandelt für einen repräsentativen Bereich viskoser Strömungen. Bei der instationären Betriebsweise werden die "Phasenänderungsschichten" in Raum und Zeit verfolgt sowie die Austrittstemperatur und die Verdampfungsrate (oder die elementare Wärmebelastung). Die stationäre Lösung liefert die Charakteristika für stabiles Betriebsverhalten. Das Verständnis beider Lösungen liefert neue Einsichten zur Bestimmung der charakteristischen Auslegungsparameter und mögliche Verbesserungen der Betriebsweise.

ТЕОРЕТИЧЕСКИЙ АНАЛИЗ СТАЦИОНАРНЫХ И НЕСТАЦИОНАРНЫХ РЕЖИМОВ РАБОТЫ ПОРИСТОГО ЭЛЕМЕНТА С ВНУТРЕННИМ ЭНЕРГОПОДВОДОМ ПРИ ФАЗОВЫХ ПРЕВРАЩЕНИЯХ И ПЕРЕГРЕВЕ ПАРА

Аннотация — Теоретически анализируются основные параметры, влияющие на режимы работы пористого реактора с внутренним энергоподводом при фазовых превращениях и перегреве пара. Исследуются три области с двухфазными границами раздела: жидкость, насыщенная паро-жидкостная смесь, а также перегретый пар. Рассматривается классический случай полого цилиндра в стационарных и нестационарных условиях течения вязкой жидкости. Изучение нестационарных условий задачи сводится к рассмотрению поверхностей раздела в пространстве и времени, температуры на выходе и расхода испаряющейся массы (или тепловой нагрузки на реактор). Стационарное решение позволяет определять характеристики стационарных режимов работы. Учет этих характеристик позволяет по-новому определить основные параметры конструкции и возможные способы улучшения характеристик.